ICAS PAPER
No. 72 – 14

HEAT TRANSFER IN SEPARATED REGIONS IN SUPERSONIC AND HYPERSONIC FLOWS

by
Josef Rom, Professor, Faculty of Aeronautical Engineering,
Arnan Seginer, Senior Lecturer,
Rimon Ariely and Michael Green, Instructors
Department of Aeronautical Engineering
Technion - Israel Institute of Technology
Haifa, Israel

The Eighth Congress of the International Council of the Aeronautical Sciences

INTERNATIONAAL CONGRESCENTRUM RAI-AMSTERDAM, THE NETHERLANDS
AUGUST 28 TO SEPTEMBER 2, 1972

Price: 3. Dfl.

HEAT TRANSFER IN SEPARATED REGIONS IN SUPERSONIC AND HYPERSONIC FLOWS*

J. Rom**, A. Seginer***, R. Ariely**** and M. Green****
Technion - Israel Institute of Technology,
Haifa, Israel.

Abstract

Heat transfer rates in separated, two-dimensional and axisymmetric, base type flows are investigated theoretically and experimentally. The theoretical evaluation is obtained by an extended Crocco-Lees integral method. An improved solution of the non-similar boundary layer flows is obtained by a finite difference-differential solution using the shooting method and leading to a prediction of the separation point by an interpolation procedure. Empirical correlation relations are presented for the effects of the Mach and Reynolds numbers, initial boundary layer thickness and model geometry on the maximum heat transfer at reattachment and its location.

I. Introduction

Flow separation may be caused either by the boundary layer retardation by an adverse pressure gradient or by an abrupt drop of the geometrical boundary. The first type of separation may be defined as the boundary-layer interaction-type separation while the second may be defined as the base type separation. The separated flow field is composed of the flow upstream of separation, the separation point, a separated region (which includes a mixing layer and a recirculating "dead water" zone), the reattachment region and the flow downstream of the reattachment. It is well known that due to the intimate interaction between the viscous shear layer and the external flow these separated flows are extremely complex for theoretical analysis and also extremely difficult for comprehensive experimental investigations. Methods for the analysis of these flows were suggested by Chapman et al[1] Korst[2], Crocco and Lees[3] and followed by many others, some of which are listed in the present references list (e.g. Refs. (4) to (8)).

It is evident that this complex problem becomes much more complicated when the heat transfer in the separated region is also considered. It was shown by Chapman[9] and also measured experimentally[10,11,12] that the heat transfer rates to the boundaries of the "dead water" zone are greatly reduced as compared to the attached flow case. However, very high heat transfer rates are measured at reattachment and beyond[10,12]. Such high heat transfer rates at reattachment were also estimated by Chung and Viegas[13]. This local increase in the heat transfer rate could easily outweigh the reduction in the heat transfer in the "dead-water" zone. The need for a theoretical evaluation of the local heat transfer rate distribution was thus clearly indicated since the previously mentioned methods evaluated mainly the average rate in the constant pressure regions[9,13]. Local heat transfer rates are obtained, rather inaccurately, primarily by the use of momentum integral methods[6] or similar moment methods[14]. Notably the best results are obtained by Holden[15] and Klineberg and Lees[16]. These works extended the Lees-Reeves method[6] by adding the integral energy equation and using a two parameter family of velocity and enthalpy profiles. In order to obtain a simpler and faster method for the evaluation of the heat transfer rates in a laminar supersonic separated boundary layer the two senior authors proposed a momentum and energy integral correlation method[17] that is an extension of the Crocco-Lees method. This method and its results are briefly outlined in Section III. The attractive feature of this method is that the velocity and enthalpy profiles do not have to be specified, and the non-uniformity of the actual velocity and enthalpy distribution across the dissipative flow is accounted for only approximately by defining appropriate velocity and enthalpy shape parameters, (κ_u) and (κ_h) respectively. This method, instead of directly satisfying the local momentum and energy equations, introduces integral conservation equations, relating the average boundary layer properties (represented by the shape parameters) to a mixing rate parameter.

The integral-correlation method derives the necessary correlation functions from "similar" boundary layer solutions, although the separated flow is definitely non-similar. When separation is caused by an adverse pressure gradient (e.g. shock-wave boundary-layer interaction) even the flow that approaches separation is non-similar. The similar solutions cannot correctly describe such flows and cannot predict the separation point. In order to obtain a better prediction of the separation point and a better heat transfer rate distribution in the separating flows the authors introduced an improved approximate numerical method for the solution of the non-similar boundary layer equation[18]. This method, described briefly in Section III, is a difference-differential method, where the streamwise gradients are replaced by backward finite differences schemes. The similar solutions are described as "memory-less" (as are also the "locally similar" solutions) and the "exact" solutions as having a full "memory". It will be shown that the present method has a "limited memory" and can therefore

* This paper is based on research which was supported in part by the Aerospace Research Laboratory, O. A.R. through the European Office of Aerospace Research, U.S. Air Force.

** Professor, Department of Aeronautical Engineering.
*** Senior Lecturer, Department of Aeronautical Engineering.
**** Instructor, Department of Aeronautical Engineering.

overcome some numerical difficulties of other non-similar methods in the calculation of heat transfer rate up to the separation point and the prediction of its position. Numerical solutions, like this method, are being applied to the separated zones and it is hoped that such solutions will enhance the calculations of local heat transfer rates in additional zones in the separated flow.

In addition to these two theoretical works, an experimental program was conducted over several years, in which the heat transfer data was accumulated in order to improve the understanding of the separated flow phenomena and in order to find correlations for the heat transfer rates. Measurements of heat transfer rates in various separated flow configurations are presented in references (10-12) and (19-22). From these results one may correlate the peak heat transfer rate that occurs at reattachment with the location of this peak. It is also found that the unit-Reynolds number is the governing parameter in the separated flow heat transfer. The most interesting conclusion is that the peak heat transfer rate in transitional reattachment is not only very much higher than the one found in laminar reattachment, but is also much higher than the peak found in the turbulent case. A possible explanation for this effect may be found in relating the large increase in the heat transfer to streamwise disturbances that are associated with the transition mechanisms and may be responsible for a very large increase in the heat transfer rate as shown in reference (23). These results are discussed in Section IV.

II. Phenomenological Description of Heat Transfer in Separated Flows

Investigations of heat transfer rates in various separated flows indicate several general features. These features must be accounted for in the models used for the analytical studies of these problems.

Ahead of separation, the heat transfer rate variation is governed by the usual boundary layer flow relations. Therefore the heat transfer rate in this region depends on the following flow characteristics: the state of the boundary layer (laminar, transitional, turbulent), Mach number, pressure gradient and the wall and the free stream conditions. The heat transfer rates in the flow far upstream of the separation point, or upto the separation point (when the flow separates abruptly because of a geometrical discontinuity), can be calculated by using the similar boundary layer solutions of Cohen and Reshotko[24]. The separating and separated boundary layer in the viscous-inviscid interaction zone can be calculated by the non-similar method [18].

In base type separated flows, the heat transfer will be equal to the undisturbed flow value practically up to the separation point at the base shoulder. Beyond separation, in the "dead water" zone, very low heat transfer values are obtained. The heat transfer rate tends to increase as the reattachment zone is approached. At reattachment one can distinguish between the purely laminar flow case at low Reynolds numbers where the heat transfer rate increases slowly and asymptotically towards the attached flat plate value, and the higher Reynolds number flow case where a peak in heat transfer rate is observed. This peak increases as the Reynolds number is increased and the flow becomes transitional. Values of up to seven times the attached laminar flow value are observed in this case[12,17]. It is interesting to note that at turbulent flow conditions peak heat transfer rates of only two to three times the attached turbulent heat transfer rate are measured[25-28].

Downstream of reattachment the heat transfer rate is found to decrease towards the attached flat plate value. At transitional conditions the heat transfer rate reduction is only partial since the flow becomes turbulent further downstream of reattachment. For the turbulent case the heat transfer is reduced towards the attached turbulent flow values.

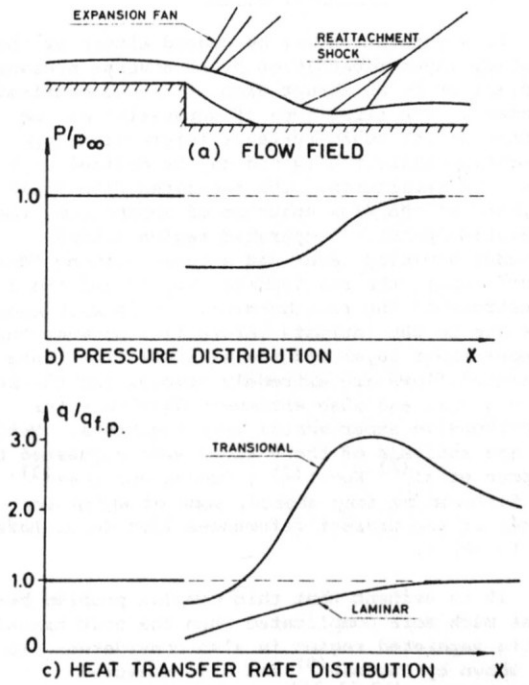

Figure 1. Heat Transfer Rates in the Various Separated Flow Fields.

These variations of the heat transfer rates in the various separated regions are shown in Fig. 1. The important parameters that characterize these heat transfer rate variations are: the value of the peak heat transfer rate $q_{max}/q_{f.p.}$, the position $(\Delta x/h)_p$ of this maximum heat transfer, the minimum value of heat transfer at separation ($q_{min}/q_{f.p.}$), the asymptotic value of heat transfer rate beyond reattachment; the average heat transfer rate in the separated region ($q_{ave}/q_{f.p.}$). All these are functions of the flow parameters: Reynolds and Mach numbers, stagnation to wall enthalpy ratio, the state of the boundary layer ahead of separation and transition effects in the

separated flow. The flow and model geometries as well as the boundary conditions in the separated region (cooling, heating, mass injection, suction etc.,) are the additional parameters that are required to define the problem.

III. Theoretical Evaluation of the Heat Transfer Rate.

Two methods for the theoretical evaluation of the heat transfer rates in the separated flow field are used by the authors. One is an integral-correlation method that solves the complete interaction field satisfying the conservation equations on the average. It will be shown that its results, though qualitatively good, have to be improved by the use of better correlation functions. The second, differences-differential method solves the local differential equations of the non-similar boundary layer. This method may furnish these required correlation functions and can also be used in an interaction program.

The Integral Correlation Method

The integral method proposed by the two senior authors in Ref. (17) is very briefly described here. Since this method is an extension of the well known Crocco-Lees method[3] and uses essentially the same notation and many of its equations, the detailed derivation of the method will not be repeated here. Only those details of the theory proposed in Ref. (17) that are essential for the discussion of the results are given here. The interested reader is advised to consult references (3) and (17) for further details.

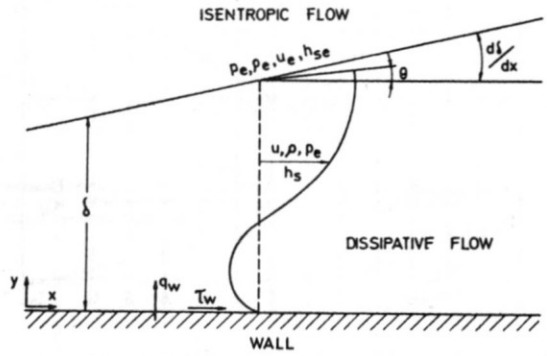

Figure 2. The Crocco-Lees Flow Model.

Basic Equations and Relations. The Crocco-Lees flow model is used (Fig. 2). A total energy flux $H = \int_0^\delta h_s \rho u dy$ is defined in addition to the previously defined[17] average fluxes of mass, $(\bar{m})$, and momentum (I), (h_s is the local total enthalpy). With these definitions, the integral conservation equations for mass and momentum are used with the addition of an integral energy conservation equation

$$dH/dx = h_{se}(d\bar{m}/dx) + \dot{q}_w \qquad (1)$$

where h_{se} is the edge total enthalpy and $\dot{q}_w$ is the heat transfer rate from the wall into the boundary layer. When an average total enthalpy $h_{s_1} = H/\bar{m}$, is added to the previously defined average velocity u_1, density ρ_1 and temperature T_1, one can relate these average properties to the boundary layer thickness δ, the displacement and momentum thicknesses, δ^* and δ^{**} respectively, and a newly defined enthalpy thickness

$$\delta^{***} = \int_0^\delta [(\rho u)/(\rho_e u_e)][(h_s/h_{se}) - 1]dy =$$

$$= [H/(\rho_e u_e h_{se})] - \delta + \delta^*$$

The relation for $u_1/u_e = \kappa_u$ and for $(\rho_1/\rho_e) = (T_e/T_1)$ can be found in Ref. (3) and the additional relation for the average total enthalpy is:

$$h_{s1}/h_{se} = T_{s1}/T_{se} = \kappa_h = (\delta - \delta^* + \delta^{***})/(\delta - \delta^*) \qquad (2)$$

κ_u is a velocity shape parameter. It is always smaller than one even in the case of the velocity overshoot experienced with a hot wall and a favorable pressure gradient. κ_h is a total-enthalpy-profile shape parameter and indicates the heat transfer conditions. For an adiabatic wall $\kappa_h = 1$ (irrespective of the Prandtl number), for a hot wall $\kappa_h > 1$, and for a cold wall $\kappa_h < 1$. A dimensionless velocity $w = u/a_{se}$ (where a_{se} is the free stream stagnation speed of sound) and several auxiliary quantities and functions are now defined:

$$\phi_e = (T_e/T_{se})(1/\gamma w_e) = \{1 - [(\gamma-1)/2]w_e^2\}/(\gamma w_e);$$

$$\phi_1 = (T_1/T_{se})(1/\gamma w_1); \tau_w = (1/2)\rho_e u_e^2 c_f; \dot{q}_w = h_{se}\rho_e u_e c_q$$

$$m = \bar{m}\, a_{se}; \rho_e u_e a_{se} = p/\phi_e; \quad \rho_e u_e^2 = (p w_e)/\phi_e.$$

c_f and c_q are the friction and heat transfer coefficients respectively. Utilizing these definitions, the equations of motion are rewritten as

$$dm/dx = \rho_e u_e a_{se}[(d\delta/dx) - \theta] = (p/\phi_e)[(d\delta/dx) - \theta] \qquad (3a)$$

$$(d/dx)(m\kappa_u w_e) = w_e(dm/dx) - \delta(dp/dx) - [(p w_e)/\phi_e](c_f/2) \qquad (3b)$$

$$(d/dx)(m\kappa_h) = dm/dx + (p/\phi_e)c_q \qquad (3c)$$

(Eqs. 3a and 3b are taken from Ref. (3) and Eq. 3c was added in Ref. (17)). Three additional relations are introduced:

The reduced mass flow $m = (p\delta)/\phi_1$ (4a)

The Bernoulli equation and the Prandtl-Meyer relation in the outer flow

$$dp/p = -(dw_e/\phi_e) \qquad (4b)$$

$$\theta = \theta(w_e) \qquad (4c)$$

Eliminating p and θ by the use of Eqs. (4b) and (4c) one obtains four independent relations for the eight unknowns; δ, m, κ_u, κ_h, w_e, c_f, c_q, ϕ_1. Four additional relations are required for the solution of the problem. The Crocco-Lees mixing

rate K is used as the fifth relation

$$d\bar{m}/dx = K\rho_e u_e \quad \text{or} \quad K = (d\delta/dx) - \theta \qquad (5)$$

This relation, however, adds the mixing coefficient K as a new unknown. A complete mathematical formulation of the problem can therefore, be obtained only if c_f, ϕ_1, K and c_q are related directly to the other five unknowns. The Crocco-Lees method[3], being adiabatic, proposed such correlations only for the first three quantities. An additional correlation for c_q is suggested here. These correlations between the various unknowns are the main disadvantage of the Crocco-Lees method as well as the present method since they must be obtained independently either from theory or experiment. When applied to separated flow the required experimental information is insufficient and the correlations that are used are based on similar solutions of the boundary layer equations.

Solution for a Constant Pressure Region: When the pressure is assumed constant (as in the dead water region in a separated flow field) it was shown in Ref. (17), that the equations, once the necessary correlations are introduced, can be solved in a closed form. It is also found that both shape parameters, which are the main variables of the present formulation of the problem, can be evaluated directly from the thicknesses of an equivalent incompressible boundary layer (that is obtained by a Dorodnitsyn type transformation) through the same relations as in the compressible flow (Eq.2). It is therefore concluded that the required correlations for K, c_f and c_q can be obtained from known incompressible solutions. The correlations for K and c_f were already given in Ref. (3). In the same way it can be shown that

$$c_q = \dot{q}_w/(h_{se}\rho_e u_e) = (\mu_e/\mu_o)c_{qi} \qquad (6)$$

where the subscript i denotes the equivalent incompressible conditions and o designates the transformation reference conditions. From the flat plate incompressible boundary layer solution we know that mass and heat fluxes are related to the Reynolds number (based on the length ξ)

$$\bar{m}_i/\mu_o = C_1(Re_\xi)^{1/2} \qquad (7)$$

$$c_{qi} = C_2(Pr)^{-2/3}(Re_\xi)^{-1/2}\,[(h_w/h_{se}) - r] \qquad (8a)$$

where r is the recovery factor and C_1 and C_2 are constants. In other laminar boundary layer solutions Eqs. (7) and (8a) retain the same form and only the values of C_1 and C_2 vary as functions of κ_u. Thus the general form of equation (8a) will be

$$c_{qi} = B(\kappa_u)(Pr)^{-2/3}[(h_w/h_{se}) - r](\mu_o/\bar{m}_i) \qquad (8.b)$$

where the heat transfer correlation function $B(\kappa_u)$ is equal to C_2/C_1. The equivalent compressible relation is obtained from Eq. (6).

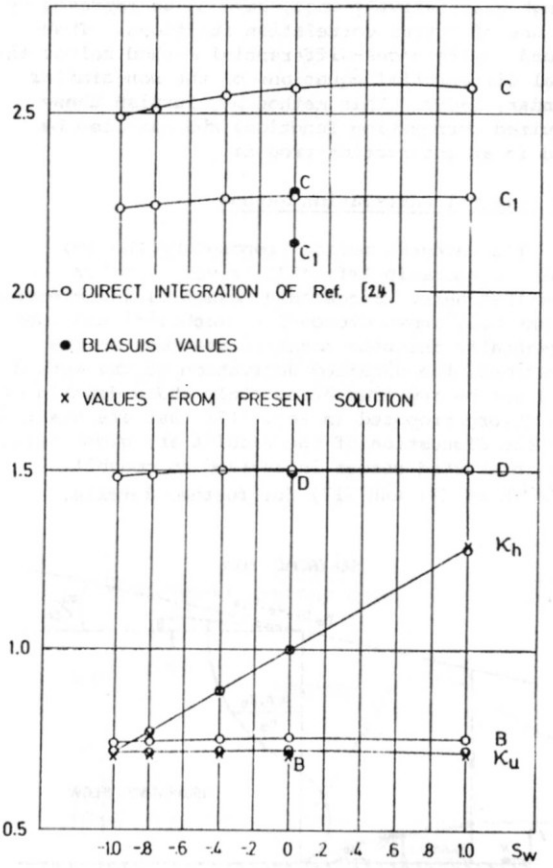

Figure 3. Flat Plate Solution and Correlation Functions.

Table 1 Comparison of Flat Plate Present Results with Blasius and Cohen-Reshotko Data

S_w	*Present results*					*Blasius results*	*Cohen-Reshotko results*	
	κ_u		κ_h					
	Blasius data [4]	*Cohen-Reshotko data* [24]	*Blasius data* $Pr = 1$	*Blasius data* $Pr = 0.723$	*Cohen-Reshotko data* $Pr = 1$	κ_u	κ_u	κ_h
−1.0	0.693	0.7024	0.6890	0.6716	0.7024	0.693	0.7167	0.7142
−0.8	0.693	0.7037	0.7512	0.7488	0.7629	0.693	0.7165	0.7673
−0.4	0.693	0.7059	0.8756	0.9033	0.8824	0.693	0.7157	0.8873
0	0.693	0.7070	1.0000	1.0578	1.0000	0.693	0.7195	1.0000
1.0	0.693	0.7071	1.3110	1.4440	1.2929	0.693	0.7165	1.2810

When the correlation functions $B(\kappa_u)$, $C(\kappa_u)$ and $D(\kappa_u)$ are known (where $C(\kappa_u)$ and $D(\kappa_u)$ are the Crocco-Lees mixing rate and the skin friction correlation functions) the flow equations (Eqs. 3a, 3b, 3c and 5) can be integrated. The solution can be obtained in a closed form for a constant wall temperature, flat plate flow. This was done both for the Blasius flow and for the Cohen-Reshotko flows[24] for several values of the wall enthalpy ratio $S_w = (h_w/h_{se}) - 1$. The values of the correlation functions in both flows are shown in Fig. (3) and the resulting shape parameters are compared in Table (1) and Fig. (3). Agreement is very good. The small differences in the results based on the Cohen-Reshotko data are due to insufficient accuracy in the graphical presentation of the data in Ref. (24).

Solution for a Varying Pressure Region. In this case the compressible boundary layer equations are transformed using the Stewartson transformation into the incompressible boundary layer equations except for the pressure gradient term in the momentum equation which is now preceded by the coefficient $h_s/h_{se} \neq 1$. It is still possible to use approximate parameters obtained from an equivalent incompressible boundary layer since the momentum equation is solved here in its integral form and the average value of (h_s/h_{se}) does not differ too much from unity. However better values for the correlation functions can be obtained from the Cohen-Reshotko similar solutions[24] since they solved the same transformed momentum equation. When the Stewartson transformation is applied to the present equations and relations, the shape parameters and the mixing rate and skin friction correlation functions are again evaluated directly from any equivalent incompressible boundary layer. Only the heat transfer correlation function $B(\kappa_u)$ must be evaluated from the equivalent Cohen-Reshotko flow, otherwise, for a general incompressible flow an error of 10% in c_q can be expected.

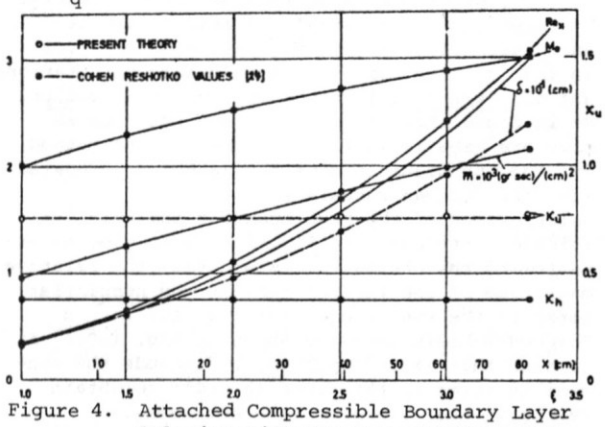

Figure 4. Attached Compressible Boundary Layer Solution with Pressure Gradient and Heat Transfer. $S_w = -0.8$; $\beta = 0.5$

When the correlation functions are known Eqs. (3a,3b,3c and 5) can again be integrated. The results of a solution of an attached similar flow are found to agree with the corresponding Cohen-Reshotko solution (Fig. 4).

Application to Separated Flow. The present method can now be applied to separated flows once the proper correlation functions are known. Out of several attempts at solutions of backward facing step separations, with various correlation functions the best results were obtained with the Cohen-Reshotko attached flow parameters in the flow up to the separation point and again downstream from reattachment, and with the Cohen-Reshotko "lower branch" (backflow) solutions in the separated region. These correlation functions are shown in Fig. (5) (for $S_w = -0.8$). It was observed, however, that the mixing rate calculated from the Cohen- Reshotko results was too low to

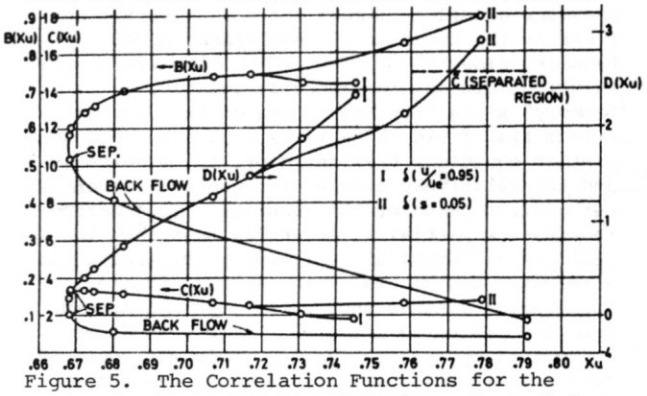

Figure 5. The Correlation Functions for the Separated Flow Solution. $S_w = -0.8$

initiate reattachment. An average, constant value of $\bar{C} = 15$ was therefore used in the separation zone as suggested by Glick[4] and confirmed by Rom[29] who found also a high value of $\kappa_u = 0.85$ immediately behind the step. This value is in good agreement with the Cohen-Reshotko backflow values for κ_u. Detailed solutions for the previously defined unknowns for several combinations of Mach and Reynolds numbers are presented in Ref. (17), and compared with the experimental data of Ref. (12). Several computed heat transfer rate distributions in the separated flow behind a backward facing step, for various Reynolds numbers are presented in Fig. (6). The comparison of these results with the experimental data of Ref. (12) presented in Fig. (7) indicates good qualitative agreement. The main quantitative differences are that the calculated heat transfer rate distributions are "stretched", or longer, compared with the measured ones. Apparently a better correlation function $B(\kappa_u)$ would improve the calculation.

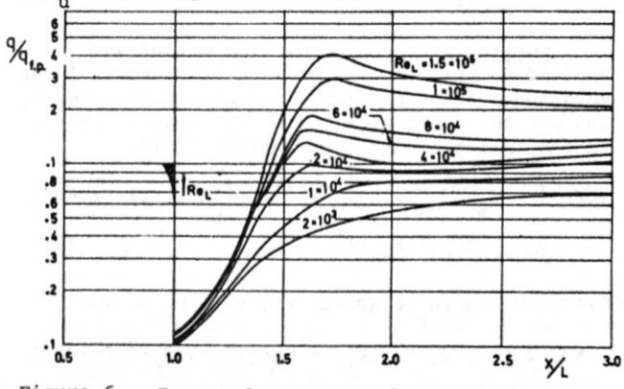

Figure 6. Computed Heat Transfer Rate Distributions Behind a Backward Facing Step.

The Finite Differences-Differential Method.

The need for a non-similar solution of the boundary layer equations was demonstrated in Section I. Since the authors intend to use the solution as part of a viscous-inviscid interaction method preference is given to the simplest method. By far the simplest methods were the "locally similar" solutions that neglected the non-similar terms in the equations at every station[30]. The flow is not similar since the solution varies along the streamwise direction because of the external pressure gradient (except for the Falkner-Skan flows or the compressible equivalent Cohen-Reshotko Flows[24]). However, these "locally similar" solutions are obtained locally and have no "memory" since they are independent of any upstream flow field characteristics. The full non-similar equations have therefore to be solved, and the relatively simple difference-differential method is chosen for the solution. This method reduces the partial differential equations to ordinary differential equations by replacing the streamwise derivatives with backward finite differences schemes that carry over the memory from the preceding stations. This method was introduced by Hartree[31] and later was extended in the many works by Smith and his co-workers. The authors generally adopted Smith's approach that has been described in many papers (e.g. 32). Only the improvements on this method are briefly outlined here while the full details can be found in Ref. (18).

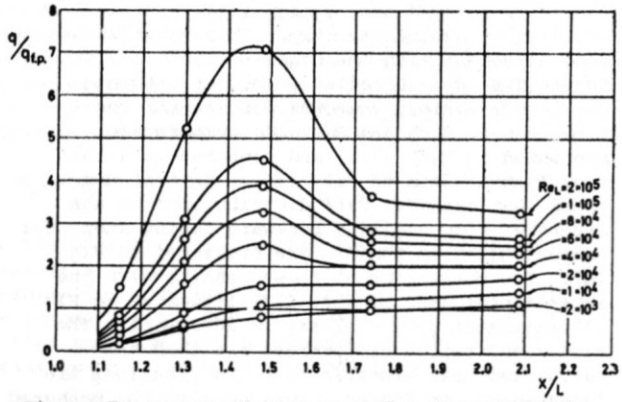

Figure 7. Measured Heat Transfer Rates Behind a Backward Facing Step in the Shock Tube (12).

Outline of the Method. The method was applied to the momentum and energy boundary layer equations, written for the stream function $f=u/u_e$ and the total enthalpy ratio function $g = H/H_e$, in the Illingworth transformation field:

$$[CF_{\eta\eta}]_\eta + C_\infty \beta[(\rho_e/\rho)-(F_\eta+1)^2]+C_\infty[(\beta+1)/2](F+\eta)F_{\eta\eta}= = C_\infty\xi[(F_\eta+1)F_{\eta\xi}-F_{\eta\eta}F_\xi] \quad (9)$$

$$\{(C/Pr)G_\eta+(u_e^2/H_e)C[(Pr-1)/Pr](F_\eta+1)F_{\eta\eta}\}_\eta + + C_\infty[(\beta+1)/2](F+\eta)G_\eta = C_\infty\xi[(F_\eta+1)G_\xi-G_\eta F_\xi] \quad (10)$$

where (ξ,η) are the transformed coordinates; $F = f-\eta$; $G = g-1$; C is the compressibility index $C = (\rho\mu)/(\rho_e/\mu_e)$; and β is the external flow pressure gradient, $\beta = (\xi/u_e)(du_e/d\xi)$. The boundary conditions are:

$$F(\xi,0) = f_w(\xi) \ (\text{or} \equiv 0); \quad F_\eta(\xi,0) = -1;$$

$$G(\xi,0) = g_w - 1 \ (\text{or } G_\eta(\xi,0) = 0); \quad F(\xi,\infty) = 0;$$

$$G(\xi,\infty) = 0 \quad (11)$$

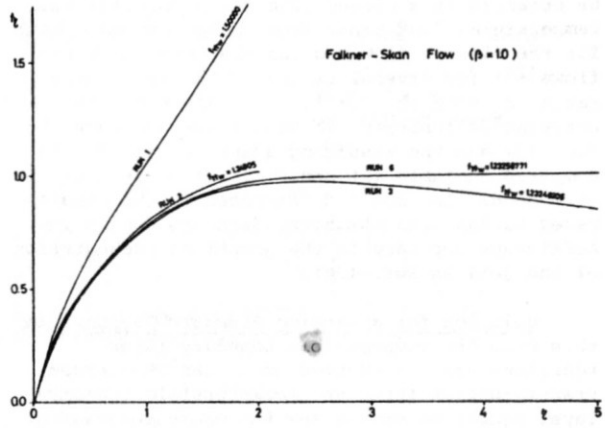

Figure 8. Typical Convergence of the Velocity Solution.

Following Smith, the streamwise derivatives are first replaced by backward finite differences schemes (two and three points differences). Then the two point boundary value problem is redefined as an initial boundary value problem using a modified version of the "shooting method" employed by Smith. Determination of the boundary layer "edge" location is improved using the Nachtsheim-Swigert method[33], and the iteration process for the correct initial conditions at the wall is facilitated by the uncoupling of the energy equation from the momentum equation and perturbing them separately by small variations in the initial conditions. A typical convergence of the iteration process is shown in Fig. (8).

The programmed equations were first checked by comparison with Smith's adiabatic results[32]. An optimum step size is determined to be: 0.01 in the η direction (100 grid points per station) and of $\Delta x/L = 0.01$ in the streamwise direction. It is found that the accuracy and the machine time are greatly in favor of the present method. For the nonadiabatic case the method is compared with the Chapman-Rubesin solution[34]. The calculations of the heat transfer and skin friction (presented in Fig. 9) are in good agreement with the Chapman-Rubesin data. The relative magnitude of the various similar and nonsimilar terms in the energy equation (Eq. 10) in the Chapman-Rubesin case are shown in Fig. (10). It is seen that it is important to include the non-similar terms in this case in order to obtain realistic heat transfer rate estimates.

Prediction of the Separation Point in Retarded Flows. When the nonsimilar formulation is applied to retarded flows the difference-differential methods have the following inherent problem. Once the finite differences scheme is introduced, the streamwise derivatives in the non-similar terms on the righthand side of Eqs. (9) and (10) are replaced by differences of the form of $(F_\xi)_n = (1/\Delta\xi)(F_n-F_{n-1})$, thus the righthand side of the equations is preceded by a $(\xi/\Delta\xi)$ factor.

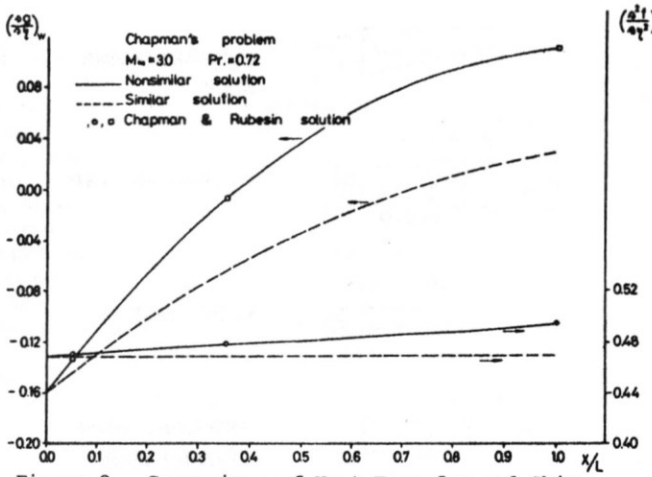

Figure 9. Comparison of Heat Transfer and Skin Friction Results with Ref. (34).

When this factor becomes too large (typical values are between 40 to 60) the numerical solutions of the equations do not converge due to a strong amplification of errors in the non-similar terms. This difficulty usually prevents the application of these methods over long flow lengths (large ξ) and also does not allow the refinement of the solution by cutting down the step size $\Delta\xi$, which is required in a retarded flow when the separation point is approached. The result is that the solution has to be stopped some distance upstream of the separation point and the location of the separation point can be estimated only by a rough extrapolation. To overcome this problem it is suggested in Ref. (18) to transform the streamwise coordinate ξ by a simple translation $\xi = (x-x_{ref})/L$. The momentum and energy equations Eqs. (9) and (10) are not changed except for the

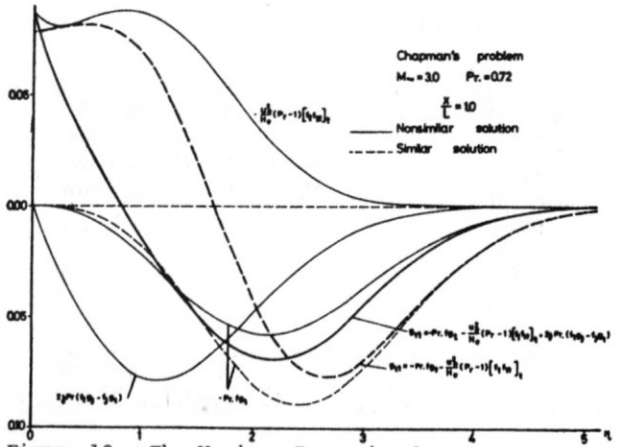

Figure 10. The Various Terms in the Energy Equation (Eq. 10).

coefficient of the non-similar terms. When $x_{ref} = 0$ one gets again the full non-similar case, and when $x_{ref} = x$ one gets the locally similar case. Such a shift of x_{ref} can prevent the appearance of the numerical problems when $(\xi/\Delta\xi)$ becomes too large. Several methods of application of this technique were investigated. The technique that was finally chosen is to solve the non-similar equations upto a certain value of $(\xi/\Delta\xi)$ (which indicates the number of stations computed) and then continue the solution with this constant value. A constant value of $(\xi/\Delta\xi)$ means that x_{ref} is shifted at every station. The first part of the solution is thus fully non-similar while the rest has an intermediate memory, i.e. it carries the same upstream information with a reduced weight which can be described figuratively as a "shortened memory". The "length of the memory", or the constant value of $(\xi/\Delta\xi)$ should be carefully chosen so as to prevent numerical instability and yet minimize the deviation from the full non-similar solution.

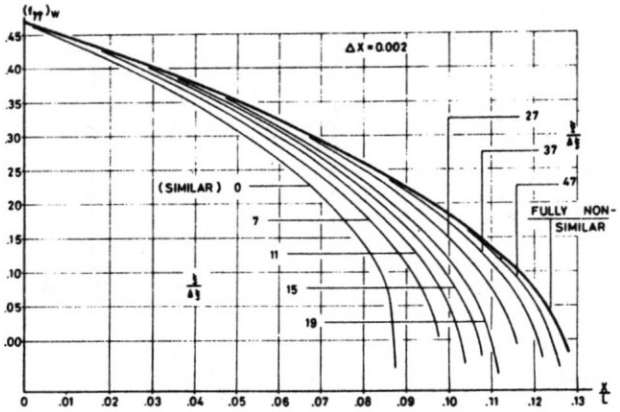

Figure 11 . Effect of the "Memory Length" $(\xi/\Delta\xi)$ on the Skin Friction Distribution.

This "shortened memory" is applied to the Howarth retarded flow defined by the external flow distribution $(u_e/u_o) = 1 - (x/L)$. The separation point position which is generally estimated at $(x_{sep}/L) \cong .125$ is shown to move, in a fully non-similar solution, between the values $(x/L)_{sep} = 0.127$ and $(x/L)_{sep} = 0.1264$ with decreasing step size in the streamwise direction from .01 to .001. The effect of the "length of the memory", or of the weight of the non-similar terms, on the skin friction distribution is investigated (Fig. 11). It has to be noted that the present method can always cross the separation point (divergence of the solution is prevented when necessary by translation of ξ) and the separation point can be determined by interpolation for zero skin friction. The locally similar solution predicted the location of the separation point at $(x/L)_{sep} = .08765$ and the fully non-similar solution predicted $(x/L)_{sep} = .12682$. All the other "shortened memory" solutions are shown between those two. At a "memory length" of approximately 2/3 (the constant value of $\xi/\Delta\xi$ is about 2/3 of the full length of the non-similar solution) the separation is located at $(x/L)_{sep} = .12625$. This value is a very good approximation of the 'exact' value. The variation of $(x/L)_{sep}$ with the length of the memory $(\xi/\Delta\xi)$ (which is the length of the flow that was solved from the fully non-similar equations) is shown in Fig. (12). The location of the separation point is seen to approach its final value asymptotically so that the "shortened memory" method is justified. Finally the solution of the Howarth-retarded flow is repeated with a smaller streamwise step size $\Delta x/L = .001$. With this value the fully non-similar solution diverges at $(x/L) \cong .114$ and the separation point cannot be reached. However if the "memory length" of the solution is restricted to $(\xi/\Delta\xi) = 110$ the solution can be continued past the separation point which is then obtained by interpolation (Fig. 13). The solutions with

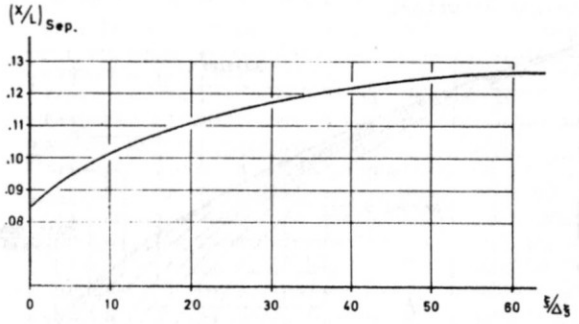

Figure 12. Variation of $(x/L)_{sep}$ with the "Memory Length". $(\Delta x/L) = 0.002$.

"shorter memories" are also shown in Figure (13). The average machine time for these calculations

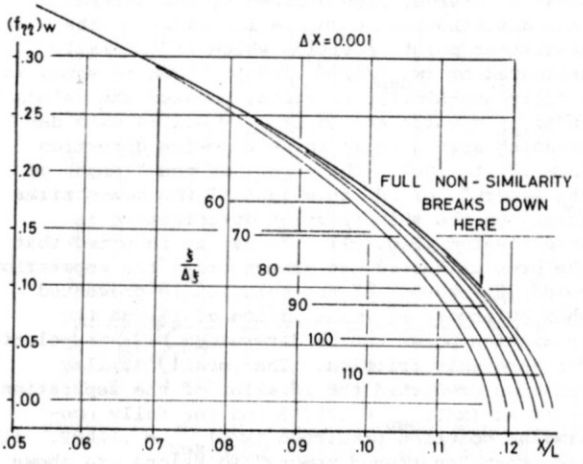

Figure 13. Convergence by "Shortened Memory". $(\Delta x/L) = 0.001$.

was less than .1 seconds per station on an I.B.M. 370/165 computer. These results compare favorably with the other solutions of the Howarth flow: a) Smith's extrapolated $(x/L)_{sep} \cong .1197$ with a machine time of 25 seconds per station on an I.B.M. 7090 computer[32]. b) The Sparrow et al[35] solution that was stopped far short of separation $(x/L \cong .095)$ and the separation point was estimated at $(x/L)_{sep} \cong .12$. c) The lower value of $(x/L)_{sep} \cong .11267$ obtained by Keller[36] in a full finite differences method with a very large step size in the x direction.

The results that were presented here indicate that the proposed method is efficient and has a sufficient accuracy. Since this method can solve the non-similar boundary layer with any prescribed pressure gradient it will be used, in conjucture with the measured pressure distributions of the separated flow field, to compute improved correlation functions for the integral method. The difference-differential method will also be coupled with an outer inviscid solution to provide an interaction method for the solution of the separated flow field.

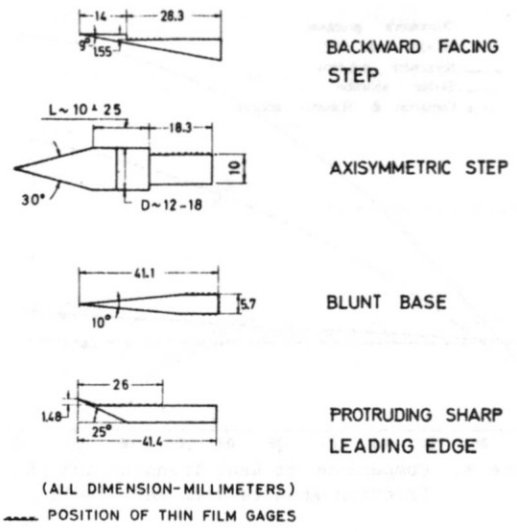

Figure 14. Separated Flow Heat Transfer Models.

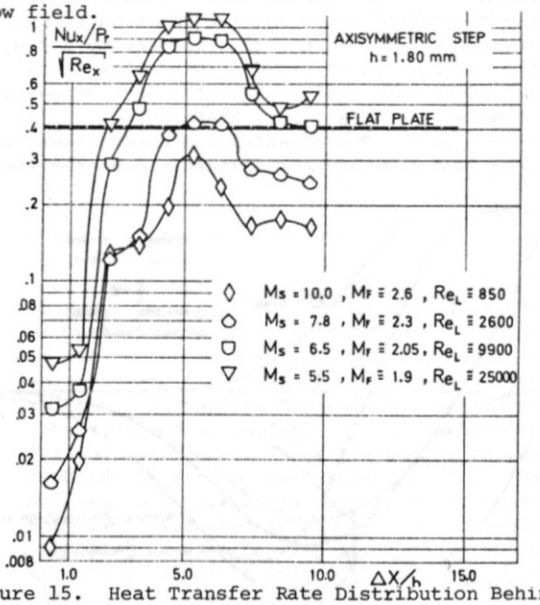

Figure 15. Heat Transfer Rate Distribution Behind an Axisymmetric Step.

IV. Correlation Relations for Heat Transfer in Separated Flow.

Previous investigations of the flow field and of the pressure variations resulted in a number of semi-empirical relations for the pressure distributions in the base type separated flows such as those of Refs. (5) and (29). The base pressure there is assumed to depend on the Mach number and the boundary layer thickness at separation. Therefore relations of the type

$$(p_b/p_\infty)_{laminar} = p_b/p_\infty[M, (h\ Re_L^{1/2}/L)] \qquad (12)$$

$$(p_b/p_\infty)_{turbulent} = p_b/p_\infty(M, h\ Re_L^{1/5}/L) \qquad (13)$$

are obtained. Explicit expressions for various flows such as backward facing steps and blunt bases are presented in reference (29). This representation is equivalent to that obtained in the "dividing streamline" formulation presented by Korst[2] as shown by Levi and Rom in Ref. (7). The pressure distributions presented by these correlations can be used in the calculations of heat transfer rates by the integral method presented in Part III. However, in the case of heat transfer rate variation even semi-empirical correlations of the type obtained in the pressure case are not available at this time.

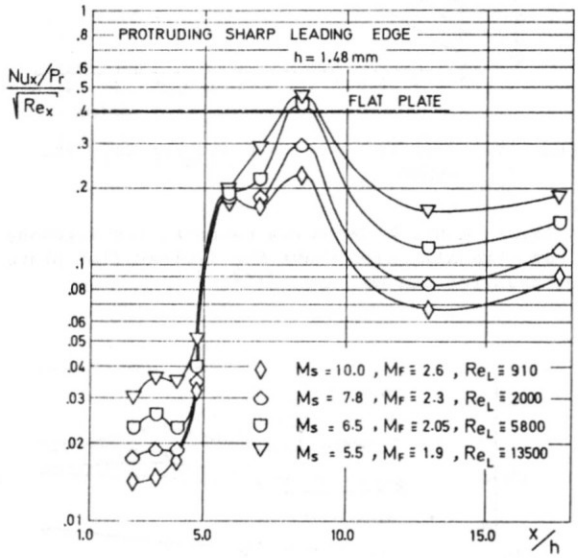

Figure 16. Heat Transfer Rate Distributions Behind a Protruding Sharp Leading Edge.

measurements of the heat transfer rates on the models shown in Fig. (14). Heat Transfer rate variations on these models are presented in Reference (21) and several typical results are shown in Figs. (7,15,16). It is shown that the peak heat transfer at reattachment can be presented by the relation

$$q_{max}/q_{f.p.} = A(hRe_L^{1/2}/L)^n \qquad (14)$$

for cases with finite boundary layer thickness at separation and

$$q_{max}/q_{f.p.} = B\ Re_h^m \qquad (15)$$

for cases with zero boundary layer thickness at separation. Values of A,n and B,m are presented in Table 2 for the various cases. The variation of the maximum heat transfer at reattachment can be correlated by the length of the mixing zone, i.e. the distance from the base to the position of this maximum. This variation is given by the relation

$$q_{max}/q_{f.p.} = C(\Delta x/h)^{-1} \qquad (16)$$

Results of a large number of investigations correlated by this relation (as shown in Fig. 17) do support this observation.

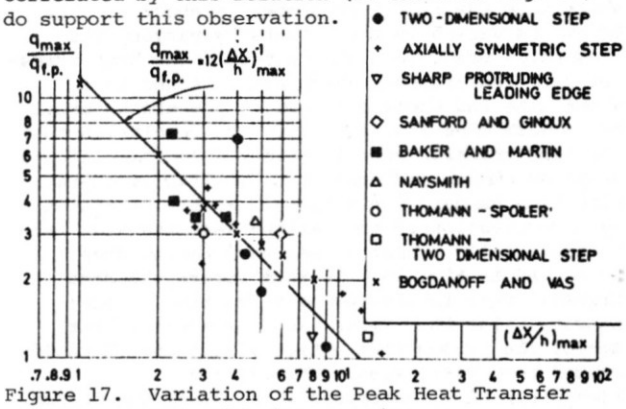

Figure 17. Variation of the Peak Heat Transfer Rate with its Location.

Table 2. Average and Maximum Heat Transfer Rate Parameters for Cases with Initial Boundary Layer and Zero Boundary Layer Thickness $q = A(hRe_L^{1/2}/L)^n q_{f.p.}$ $q = B(Re_h)^m q_{f.p.}$

	$q_{ave}/q_{f.p.}$		$q_{max}/q_{f.p.}$	
	A	n	A	n
Two-Dimensional Backward Facing Step	0.02	1.2	0.0465	1.3
Axially Symmetric Backward Facing Step	0.037	1.0	0.068	1.0
Two-Dimensional Blunt Base	0.018	0.77	0.034	0.7
	B	m	B	m
Sharp Protruding Leading Edge	0.04	0.27	0.057	0.34

Heat Transfer Rates at Reattachment to a Surface.

The heat transfer correlations are based on the measurements performed during a number of investigations in the Technion-Aeronautical Engineering Laboratories, reported in References (12, 19-22). These investigations included

The effect of the unit Reynolds number on the heat transfer rate distribution is shown in Fig. (18). The heat transfer rate parameter, $(Nu_x/Pr)/cm$, for an axially symmetric backward facing step is plotted as a function of Re/cm for each of the ten gage positions behind the step. This data is

representative of the heat transfer measurements obtained in our tests. The results illustrate the presence of the low heat transfer rates in the dead water region and the high rates in the reattachment region. It is interesting to note the variation of the heat transfer rate at the different positions behind the separation point. In the dead water regions the heat transfer rate rises slowly at the lower values of Re/cm and rapidly at the higher values of Re/cm, beyond reattachment the opposite trend is observed. This results in a "concave" variation in the dead water region and a "convex" variation in the reattachment region. The region in which the curve shape changes, that is, where an approximately linear variation is observed, marks the differentiation between the zone of "unattached" heat transfer and that of the "reattached" flow. In the present model this occurred at gage 3 position (approximately 4.45 mm from the separation point). It should be mentioned that this is not the point at which the maximum heat transfer rate occurred. The range of Re/cm which applies to the shock tube tests and that which applies to the shock tunnel tests is also indicated on Fig. (18). It should be noted that in the shock tunnel experiments the flow Mach number is 5.5, while in the shock tube the flow Mach number is about 2. The Re/cm is varied in these tests by varying the stagnation pressure. The fact that the heat transfer rate measurements which are obtained in the shock tube and those obtained in the shock tunnel match each other, does justify the conclusion that the heat transfer rate is mainly a function of unit Reynolds number and depends only slightly on the flow Mach number. This fact is well illustrated by the variation of the maximum heat transfer rate on the axially symmetric backward facing step presented in Fig. 19. In this figure the heat transfer rate is plotted as a function of step height, using the Re/cm as a parameter. Here again, the predominant effect of the unit Reynolds number is clearly seen. The value of $[(Nu_x/Pr)/cm]_{max}$ increases with increasing Re/cm. The values of heat transfer rate for the case of zero step height are indicated on this figure showing that for all except the lower value of Re/cm (2.5×10^3) the maximum value of the separated flow reattachment heat transfer rate is higher than for the equivalent nonseparated flow.

Examination of the heat transfer data obtained both in the separated flows and in the zero step height cases indicate that as the flow Reynolds number is increased the heat transfer rate increases above the expected laminar, $Re^{1/2}$ variation. It seems plausible that this increase is due to effects of streamwise disturbances which are generated by the streamline curvature in the mixing and reattaching flows. The effects of streamwise disturbances on local heat transfer to the cylindrical surface of a cone-cylinder model with attached flow is presented in Ref. (23). This effect of the streamwise vortices is shown to increase the heat transfer according to the following relation:

$$q = q_{f.p.}(1 + NRe_L) \qquad (17)$$

where N is determined by the flow characteristics or its value can be obtained from the experimental data.

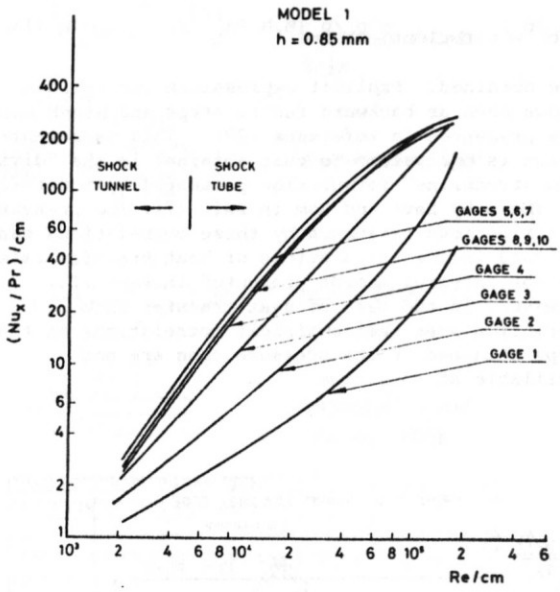

Figure 18. Heat Transfer Rate (Nu_x/Pr cm) vs. Re/cm.

For large values of Reynolds numbers, the increase of heat transfer rate above the laminar flat plate heat transfer can be large[12,22,23].

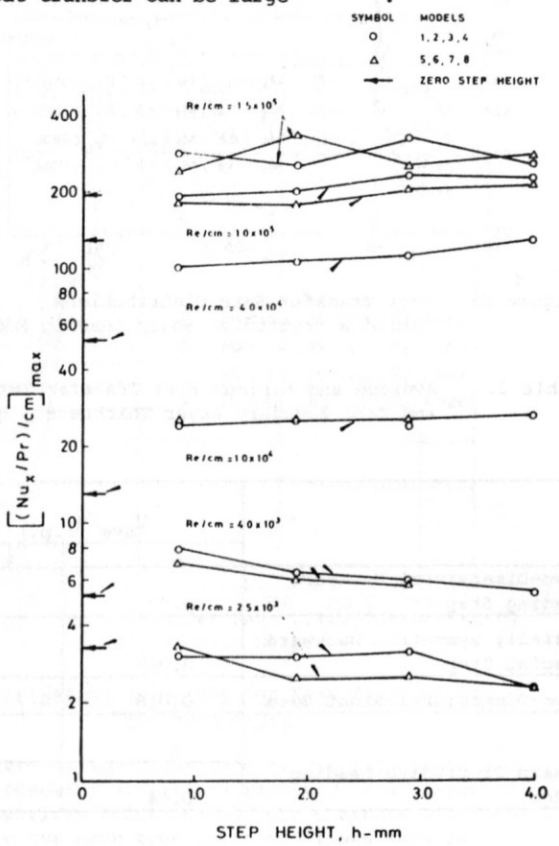

Figure 19. Maximum Heat Transfer Rate as a Function of Step Height.

Heat Transfer Rate to a Blunt Base

The heat transfer to the blunt base for laminar and transitional flows was measured in the shock

tube and the results are presented in Ref. (20). In this case the reattachment of the separated shear layer to a solid surface which dominates the heat transfer distribution in the previously described step configuration is eliminated. It is found that in a completely laminar wake flow a peak in heat transfer rate is found at the base center and the heat transfer rate is decreasing towards the base edges. This peak in heat transfer is found to depend on the boundary layer thickness parameter ($hRe_L^{1/2}/L$) similar to the relation (14) and the corresponding values of the correlation coefficients are included in Table 2.

This regular heat transfer rate distribution is distorted at higher Reynolds numbers as effects of transitional disturbances appear. As the higher Reynolds numbers additional off-center peaks are observed as indicated in Fig. (20). It is interesting to note that qualitatively similar heat transfer rate distributions were observed by Gardon and Akfirat[37] in the impinging jet heat transfer measurements when transition was artificially induced. Apparently the flow in the base region near the base stagnation zone is somewhat like the impinging jet flow. It can be also expected that in the near wake flow, three dimensional disturbances will be induced when the Reynolds number is increased. This should affect the heat transfer rate similar to the effects found in the impinging jet case. The experimental results indeed support this analogy.

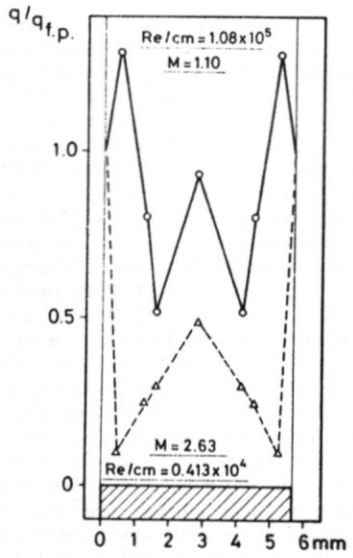

Figure 20. Heat Transfer Rates to a Blunt Base.

V. Discussion and Conclusions

The measurements of heat transfer in separated flows indicate that the heat transfer rate distribution is dominated by the high rates which are encountered at and near the impingement of the reattaching mixing layer or at the rear stagnation region for the blunt base configuration. The highest increase is found for the transitional case. It is further observed that the height of the peak in the heat transfer rate at reattachment is inversely proportional to the length from the separation point to the position of this peak. It is interesting to note that the base pressure is found to decrease as the length of the mixing zone is decreased (Ref. 5,29). Furthermore, the base pressure has it lowest value at transitional reattachment, that is, when transition occurs in the mixing layer between the separation point to the reattachment point. We find that at these conditions the heat transfer peak at reattachment is probably at its highest value.

Since the heat transfer is determined by the interaction of the separated flow field (including the external rotational flow and the mixing layer) with the viscous layer generated on the solid boundaries two methods of analytical formulation are studied.

A momentum and energy integral formulation is shown to enable the evaluation of the heat transfer rate variation in the separated flow provided that the proper correlation functions are known. It is shown that by reasonable arguments, a set of correlation parameters can be selected and the results of the calculations can be accepted to be at least in qualitative agreement with the measurements.

A more promising method for a theoretical solution is introduced in this paper. Using a finite difference-differential solution of the boundary layer equations, a solution for the non-similar flows is obtained. The problem of the numerical convergence of the solution is solved by the introduction of a reference length. It is shown that this reference length, in essence, defines a "limited memory" of the solution to the non-similar boundary layer equation. A proper choice of a "memory" length, enables a solution such that on one hand the non-similar nature of the boundary layer is preserved and on the other hand the numerical solution still converges. The present solution can be included in an iterative calculation with the external rotational supersonic characteristics solution and thus this synthesis will define a reasonably complete theoretical solution of separated flow with heat transfer.

References

1. Chapman, D.R., Kuehn, D.M., and Larson,H.K., "Investigation of Separated Flows in Supersonic and Subsonic Stream with Emphasis on the Effects of Transition", NACA Rep.1356, 1958.
2. Korst, H.H., Chow, W.L. and Zumwalt, G.W., "Research on Transonic and Supersonic Flow of a Real Fluid at Abrupt Increase in Cross Section", University of Illinois, Mech.Eng.Dept.,M.E.Tech. Rep.392-5 AFOSR TR 60-74,Dec.1969.
3. Crocco,L. and Lees, L.,"A Mixing Theory for the Interaction Between Dissipative Flows and Nearly Isentropic Streams",J.Aero,Sci., Vol.19,No.10, Oct.1952,pp.649-679.
4. Glick, H.S., "Modified Crocco-Lees Mixing Theory for Supersonic Separated and Reattaching Flows", J.Aero.Sci., Vol.29,No.11, Nov.1962,pp.1238-1244.
5. Rom, J., "Theory for Supersonic,Two-Dimensional, Laminar Base Type Flows using the Crocco-Lees Mixing Concepts",J.Aero.Sci.,Vol.29,No.8, Aug. 1962,pp.963-968.
6. Lees,L. and Reeves,B.L.,"Supersonic Separated and Reattaching Laminar Flows:General Theory and Application to Adiabatic Boundary Layer/Shock

Wave Interaction",AIAA J.Vol..2,No.11,Nov.1964, pp.1907-1920.
7. Rom, J. and Levi, E., "The Semi Empirical Parameters Used in the Dividing Streamline and the Momentum Integral Analvses for Separated Flows", Israel Journal of Technology,Vol.7,No.1-2,March 1969, pp.163-171.
8. Weiss, R.F. and Weinbaum, S., "Hypersonic Boundary Layer Separation and the Base Flow Problem",AIAA,J.,Vol. No.8,Aug.1966,pp.1321-1330.
9. Chapman,D.R., "A Theoretical Analysis of Heat Transfer in Regions of Separated Flow",NACA TN 3792, 1956.
10. Larson,H.K.,"Heat Transfer in Separated Flows", J.Aero. Sci., Vol. 26,No.12, Dec.1959,pp.731-738.
11. Bogdonoff, S.M. and Vas, I.E., "Some Experiments on Hypersonic Separated Flows",ARS,J.,Vol.32, No. 10, Oct.1962,pp.1564-1572.
12. Rom,J. and Seginer, A.,"Laminar Heat Transfer to a Two-Dimensional Backward Facing Step from the High Enthalpy Supersonic Flow in the Shock Tube", AIAA,J.,Vol.2,No.2,Feb.1964,pp.251-255.
13. Chung,P.M. and Viegas J.R., "Heat Transfer of the Reattachment Zone of Separated Laminar Boundary Layers", NASA TN-D 1072,1961.
14. Abbott,D.E.,Holt,M.and Nielsen,J.N.,"Studies of Separated Laminar Boundary Layers at Hypersonic Speed with some Low Reynolds Number Data", AIAA Paper 63-172,1963.
15. Holden,M.S.,"An Analytical Study of Separated Flow Induced by Shock Wave-Boundary Layer Interaction", NASA CR-600,1966.
16. Klineberg,J.M. and Lees, L.,"Theory of Laminar Viscous-Inviscid Interactions in Supersonic Flows", AIAA Journal,Vol.7,No.12,Dec. 1969, pp.2211-2221.
17. Seginer, A. and Rom, J., "An Integral Method for the Calculation of Heat Transfer Rate in Laminar Supersonic Separated Flows", Israel Jr. of Technology, Vol.6,No.1-2,Feb.1968,pp.72-83. Proc. X Israel Ann.Conf.Aviation & Astronautics.
18. Ariely, R., "Nonsimilar Solutions of Boundary Layer Flows with Heat Transfer and Pressure Gradient",M.Sc.Thesis, Aero.Eng.Dept. Presented to the Senate of the Technion-Israel Inst. of Tech.July 1971.
19. Rom,J. and Seginer,A.,"Laminar and Transional Heat Transfer in the Two-Dimensional Separated Flow Behind a Sharp Protruding Leading Edge", TAE Rep.71,Technion-Israel Inst.Tech.July 1967.
20. Rom,J. and Seginer, A., "Laminar Heat Transfer to a Two-Dimensional Blunt Base from the High Enthalpy Flow in the Shock Tube", Proc. 9th Israel Ann. Conf. on Aviation & Astronautics, Israel Jr. of Tech., Vol. 5, No. 1, Feb. 1967.
21. Rom, J., Seginer, A. and Green M., "Investigation of Heat Transfer in Base Type Supersonic Laminar and Transitional Separated Flows", TAE Report No. 111, Technion-Israel Inst. Tech., April 1970.
22. Green, M. and Rom, J., "Measurements of Heat Transfer Rates Behind Axially Symmetric Backward Facing Steps in the Shock Tube and Shock Tunnel", TAE Report No. 127,Technion-Israel Inst. of Tech., May 1971.
23. Small, R.D., and Rom, J., "Effect of Transverse Disturbances on Heat Transfer in a Laminar Axisymmetric Boundary Layer", TAE Report No. 146, Technion-Israel Inst. of Tech., Feb.1972.
24. Cohen, C.B. and Reshotko, E., "Similar Solutions for the Compressible Laminar Boundary Layer with Heat Transfer and Pressure Gradient", NASA Rep.1293, 1956.
25. Baker, D.J. and Martin, B.W., "Heat Transfer in Supersonic Separated Flow Over a Two-Dimensional Backward Facing Step", International Journal of Heat and Mass Transfer, Vol.9, 1965, pp.1081-1088.
26. Naysmith,A., "Measurements of Heat Transfer in Bubbles of Separated Flow in Supersonic Airstreams", ASME and Inst. of Mech. Eng.London, Int.Heat Transfer Conf.Part II ,No.43,p.378, 1961.
27. Thomann,H.,"Measurements of Heat Transfer and Recovery Temperature in a Separated Flow in a Mach Number of 1.8",FFA Rep.82,The Aero.Res.Inst. of Sweden,1959.
28. Sanford,J. and Ginoux, J.J.,"Laminar,Transitional and Turbulent Heat Transfer Behind a Backward Facing Step in Supersonic Flow", T.N.38, von-Karman Inst.for Fluid Dynamics,Belgium, Oct.1968.
29. Rom,J.,"Analysis of the Near Wake Pressure in a Supersonic Flow Using the Momentum Integral Method", Journal of Spacecraft and Rocket,Vol. 3 , No.10, Oct.1966, pp. 1504-1509.
30. Kemp, N.H., Rose,P.H. and Detra,R.W.,"Laminar Heat Transfer Around Blunt Bodies in Dissociated Air",J.Aerospace Sciences,Vol.26, No.7,July 1959,pp.421-430.
31. Hartree, D.R. and Womersley, J.R., "A Method for the Numerical or Mechanical Solution of Certain Types of Partial Differential Equations", Proc.Roy.Soc.,Vol.161A,Aug.1937, p.353.
32. Smith,A.M.O. and Clutter,D.W.,"Machine Calculation of Compressible Boundary Layers", AIAA Journal,Vol.3,No.4,April,1965,pp.639-647.
33. Nachtsheim,P.R. and Swigert,P., "Satisfaction of Asymptotic Boundary Conditions in Numerical Solution of Systems of Nonlinear Equations of Boundary-Layer Type", NASA TN D-3004,Oct.1965.
34. Chapman, D.R. and Rubesin,M.W., "Temperature and Velocity Profiles in the Compressible Laminar Boundary Layer with Arbitrary Distribution of Surface Temperature", J.Aero. Sci., Vol. 16, No. 9,Sept.1949,pp.547-565.
35. Sparrow,E.M.,Quack,H. and Boerner, C.J., "Local Nonsimilarity Boundary Layer Solution", AIAA Journal,Vol.8, No. 11, Nov.1970.pp.1936-1942.
36. Keller,H., "Accurate Numerical Method for Boundary Layer Flows", Proc. of the 2nd Int. Conf. on Numerical Methods in Fluid Dynamics, Univ. of California,Sept.15-19,1970.pp.92-100.
37. Gardon,R. and Akfirat, J.C.,"The Role of Turbulence in Determining the Heat Transfer Characteristics of Impinging Jets",Intern.J. Heat and Mass Transfer,Vol.8,pp.1261-1272, 1965.